SAND2022-8242C

DFNE 22–0007

Effects of Fracture Transmissivity Relationship on Repository Performance Characteristics

Smith, M., Portone, T. and Swiler, L.
Sandia National Laboratories, Albuquerque, New Mexico, USA

ABSTRACT: When simulating flow and transport through sparsely fractured rocks in Earth's subsurface, discrete fracture network (DFN) modeling has become the alternative approach to continuum approaches. In this work, DFNs are generated using dfnWorks, a parallelized computational suite developed by Los Alamos National Laboratory. The DFNs are then mapped to an equivalent continuous porous medium (ECPM) to allow for nuclear waste repository performance assessment simulations. To this end, reactive flow and transport calculations are performed in PFLOTRAN, a parallel multiphase flow and reactive transport code. For this study, the application problem is a crystalline repository reference case based on the Forsmark site in Sweden. When converting the fracture networks into ECPMs, fracture transmissivity is used to determine the continuum permeability field. New capabilities in dfnWorks have enabled the use of the depth-dependent correlated relationship. To understand the effect of adding the depth-dependent relationship, this study compares repository performance quantities of interest and ECPM permeabilities from the same DFN where the only change is the transmissivity relationship. It was found that although the permeabilities for the varying transmissivity relationships were significantly different, this did not strongly influence the quantities of interest.

1. INTRODUCTION

When considering the underground storage of nuclear waste in generic repositories, there must be post-closure performance assessments to provide reasonable assurance that a repository system will achieve sufficient safety and meet the relevant requirements for the protection of humans and the environment over a prolonged period of time (IAEA, 2012; NEA, 2013; Rechard et al., 2014). Within these assessments it is especially important to identify the expected concentration of radionuclides in groundwater and subsurface/waste storage properties that are most important to repository performance. In order to estimate these, many factors are studied with one of the most important being subsurface multiphase flow and transport.

When simulating flow and transport through sparsely fractured rocks in the subsurface, discrete fracture network (DFN) modeling has become the alternative approach to continuum approaches (Hyman et al., 2015). Continuum approaches use effective parameters to include the influence of fractures on the flow while the network of fractures in the DFN approach is represented as lines in two dimensions or planar polygons in three dimensions. In this work, DFNs are generated using dfnWorks, a parallelized computational suite developed by Los Alamos National Laboratory (Hyman et al., 2015). The DFNs are then mapped to an equivalent continuous porous medium (ECPM) using the open-source tool mapDFN, which allows for nuclear waste repository performance assessment simulations of coupled heat and fluid flow and reactive radionuclide transport in both porous media and fractured rock (Stein et al., 2017). These simulations are performed using PFLOTRAN, a parallel multiphase flow and reactive transport code (Lichtner and Hammond, 2012).

For this study, the application problem is a crystalline repository reference case with host rock properties comparable to the Forsmark site in Sweden (Joyce et al., 2014). The fractures are assumed to be circular in shape and are parametrized in terms of their radius and orientation, the fracture intensity (P_{32}) [m^2/m^3], and the relationship between fracture transmissivity and fracture size (radius).

Fracture transmissivity is used to determine the continuum permeability field of the ECPM, as described in Stein et al., 2017. The crystalline reference case initially assumed a single "correlated" transmissivity relationship for the entire computational domain, using a parameterization provided for the Forsmark site in Joyce et al., 2014. The "correlated" relationship is defined as

$$T = ar^b \quad (1)$$

where r is the fracture radius, T is the transmissivity, and a and b are parameter values that were fit to data.

Sandia National Laboratories is a multimission laboratory managed and operated by National Technology & Engineering Solutions of Sandia, LLC, a wholly owned subsidiary of Honeywell International Inc., for the U.S. Department of Energy's National Nuclear Security Administration under contract DE-NA0003525.

However, Joyce et al., 2014, provided parameterizations for the correlated transmissivity relationship based on depth. New capabilities in dfnWorks enabled the use of the depth-dependent correlated relationship for the crystalline reference case. A comparison of the original and depth-dependent relationships is shown in Table 1.

Table 1. Transmissivity relationship parameterizations comparison.

Depth (meters below sea level)	Transmissivity Relationship	
	Correlated, $T = ar^b$	
	Constant over domain (a,b)	Depth-dependent (a,b)
0-200	(1.6E-9, 0.8)	(6.7E-9, 1.4)
200-400		(1.6E-9, 0.8)
>400		(1.8E-10, 1.0)

To understand the effect of adding depth-dependence to the transmissivity relationship, this study compares ECPM properties and repository performance quantities of interest for each relationship. The underlying DFN is fixed so that the only difference to the system is the transmissivity relationship.

2. APPROACH

To complete this analysis and understand the effect of adding depth dependence to the transmissivity relationship, 20 DFNs were randomly generated. The two transmissivity relationships were applied to each DFN and used to construct 40 ECPMs, 20 for each relationship. To reiterate, all parameters needed to construct the ECPMs were fixed except for the transmissivity relationship parameterizations shown in Table 1. The ECPMs were then used in PFLOTRAN simulations of the crystalline repository reference case which is shown in Figure 1.

The reference case is split into three depth zones (dz1, dz2, and dz3) with a glacial aquifer positioned at the top 15 meters of depth zone one and the repository located at the top of depth zone three. The computational domain spans 3000 meters in the x direction, 2000 m in the y direction, and 1260 meters in the z direction. Three mass flow rates characterizing transport properties of the system were considered in this analysis and are also shown in Figure 1.

The continuum permeability fields from the ECPMs were separated based on depth zone and the arithmetic mean of the permeability tensor components in the x, y, and z directions were computed and denoted k_{xx}, k_{yy}, and k_{zz}. The geometric mean over mean tensor components for each depth zone was computed and denoted:

$$k_{gm} = \sqrt[3]{k_{xx}k_{yy}k_{zz}} \qquad (2)$$

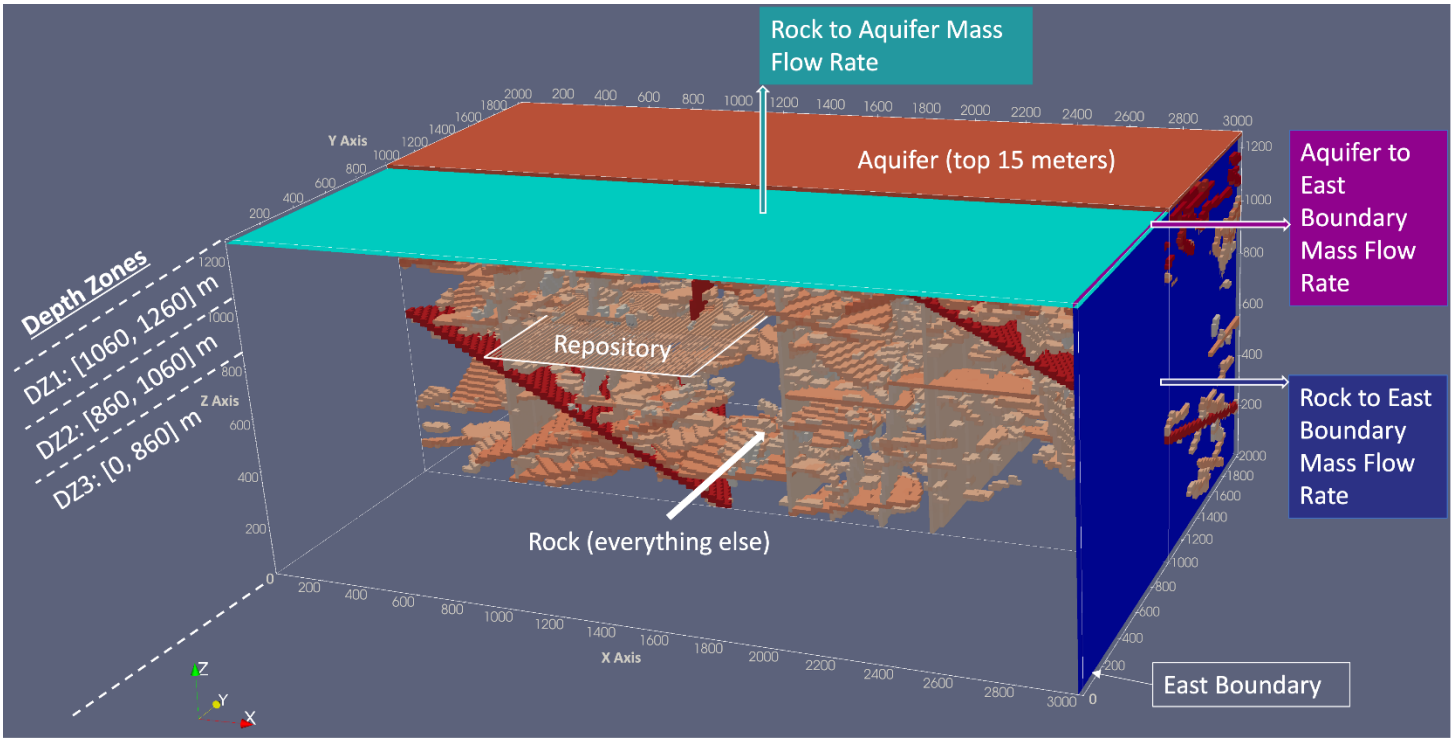

Figure 1. Crystalline repository reference case.

The specific repository performance quantities of interest (QoIs) assessed were the following:

- Maximum ^{129}I concentration in the aquifer
- Repository median residence time (MdRT) in years
- Fractional mass flux from the repository at 3 thousand years
- Mass flow rate from the rock to the aquifer
- Mass flow rate from the rock to the east boundary

The MdRT and fractional mass flux QoIs are computed by tracking the concentration of a tracer in the repository region as a function of time. This tracer is injected into the region at the beginning of the simulation, so the rate at which it is flushed from the repository provides a measure of repository performance. The MdRT is the time at which half the tracer remains in the repository region. Further details of how all QoIs are computed is provided in (Mariner et al., 2020).

For the comparative analysis, the specified QoIs were visually compared using information such as main effects plots and box plots. The primary goal was to determine if the results using the 20 DFNs with the correlated constant (CC) transmissivity relationship were significantly different from the results using the 20 DFNs with the correlated depth dependent (CDD) transmissivity relationship.

3. RESULTS

This analysis compares mean permeabilities and repository performance QoIs between the two transmissivity relationships (correlated constant vs. correlated depth-dependent). The information shown in the subsequent tables and plots is representative of all 40 cases, 20 for the correlated constant (CC) relationship and 20 for the correlated depth-dependent (CDD) relationship: outliers were not removed. Interval plots were used to examine the mean values for each type of data and the associated 95% confidence interval on the means computed over the 20 samples for each relationship. Lack of overlap in the confidence intervals indicates the CDD transmissivity relationship influenced the results significantly. To give better interpretation of what the interval plots (also called "main effects" plots) are indicating, boxplots were constructed to show the actual spread of the data for each transmissivity relationship. These plots are treated similarly to interval plots, and the level of overlap between the groups indicates the amount of influence the transmissivity relationship had on the results.

3.1. Permeability

Table 2 shows the mean k_{gm} for each depth zone computed over the set of 20 DFNs. This information shows that for all three depth zones, there is a considerable difference between transmissivity relationships. Note that the mean values of the k_{gm} for dz1 and dz2 are one to two orders of magnitude greater for the CDD relationship relative to the CC relationship.

Table 2. Geometric mean permeability comparison.

Transmissivity Relationship	dz1	dz2	dz3
CC	3.47E-16	3.12E-16	2.65E-16
CDD	1.15E-14	1.64E-15	2.36E-16

In contrast, the mean correlated constant k_{gm} is higher than the depth-dependent k_{gm} for dz3. But the absolute magnitude of this difference is quite small for dz3: about 3.0E-17 Most of these observations are to be expected considering the difference between the transmissivity relationships detailed in Table 1—in dz1, the CDD relationship assigns greater transmissivity for the same fracture size relative to the CC relationship, while in dz3 it assigns lower transmissivity for the same fracture size. However, the parameterizations for dz2 are identical. The order of magnitude difference in permeability between the transmissivity relationships is due to large fractures with centroids in dz1 extending into dz2. Transmissivity is assigned by the location of the center of the fracture and applies to the entire fracture, so the higher transmissivity of these dz1 fractures extending into dz2 influences the permeability for dz2. A final observation was that the CC transmissivity relationship had permeability values of the same order of magnitude in the *x, y,* and *z* directions. In contrast, for the CDD transmissivity relationship, the *x* and *y* directions of the permeability tensor were larger than the *z* direction by two and one orders of magnitude, respectively, for both depth zones one and two. Given this information, it is expected that there will be an increase in downstream flow and little increase in vertical flow towards the aquifer for the CDD transmissivity relationship.

3.2. Maximum ^{129}I in the Aquifer

As is shown in Figure 2, the confidence intervals for the two transmissivity relationships overlap significantly. Additionally, the confidence intervals are quite large, indicating high variance in the mean estimates for both transmissivity relationships. Based on this information, it is not accurate to say the transmissivity relationship is statistically significant for the maximum ^{129}I concentration in the aquifer.

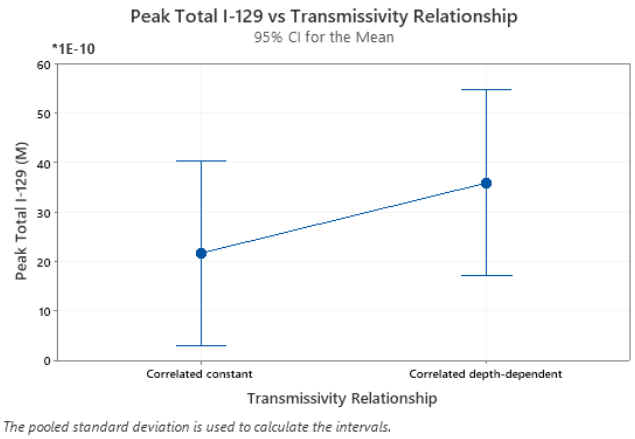

Figure 2. Interval plot for the scaler maximum ^{129}I concentration [M] in the aquifer after 1 million years.

The results shown in Figure 3 below further solidify the conclusions made from the results in Figure 2. The range of the maximum ^{129}I data is fairly consistent between the CC and CDD relationships. The depth-dependent case has a slightly higher median, and its distribution is not quite as skewed as the correlated constant case. However, there is one outlier in the depth-dependent case with a value of 2.50E-8 M, where the other results are mostly below 7.50E-9 M. This outlier can significantly increase and influence the mean estimate as shown in Figure 2. Without the outlier, the means of these two datasets would be closer.

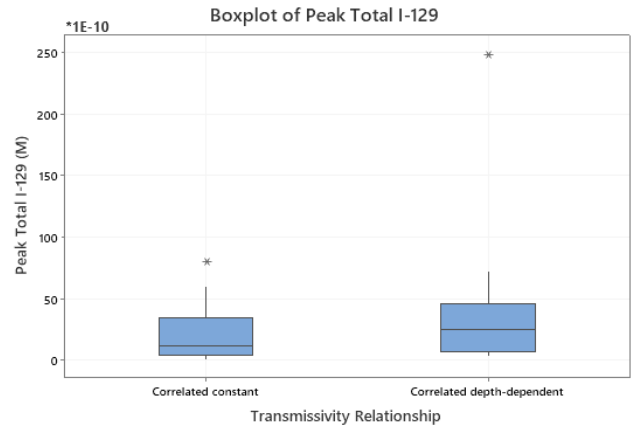

Figure 3. Box plot showing the scaler maximum 129I concentration [M] in the aquifer after 1 million years.

Figures 2 and 3 represent the maximum ^{129}I concentration in the aquifer computed over space and time, while Figures 4 and 5 represent the maximum ^{129}I concentration in the aquifer as a function of time. As shown in Figure 5, for the most part, the 95% confidence intervals overlap with the CDD relationship being slightly higher. However, this is largely influenced by the extreme outlier shown in Figure 4 which is the same outlier shown in Figure 3.

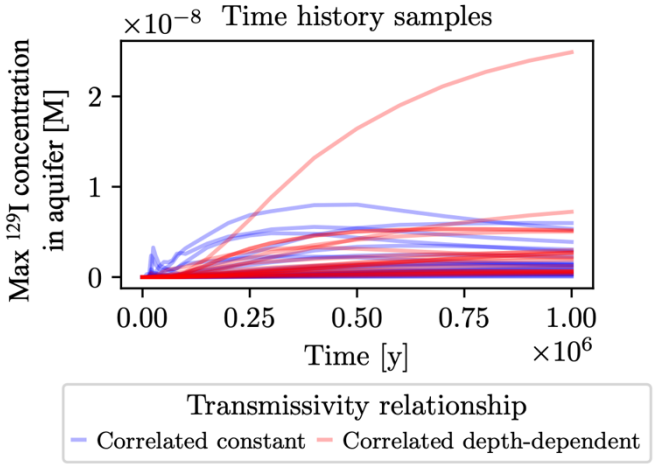

Figure 4. Maximum ^{129}I concentration [M] in the aquifer over time.

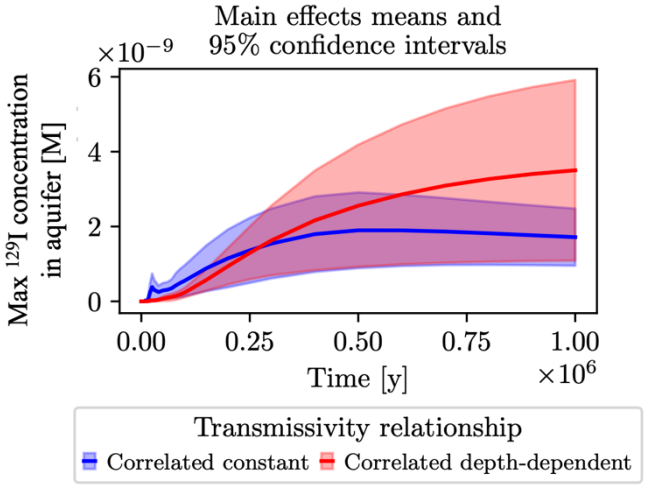

Figure 5. Main effects plot for the maximum ^{129}I concentration [M] in the aquifer over time.

3.3. Repository Median Residence Time

As shown in Figures 6 and 7, the results for the MdRT follow the same trend as the maximum ^{129}I results. There is less of an overlap between the confidence intervals in Figure 6, but the overlap in Figure 7 shows that the CDD relationship did not have a statistically significant effect on this QoI. This can likely be attributed to the small difference in permeability in depth zone three for the two transmissivity relationships.

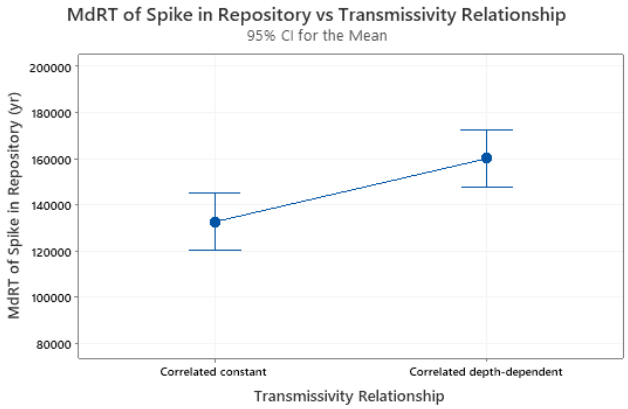

Figure 6. Interval plot for the time when half the tracer is gone from the repository in years.

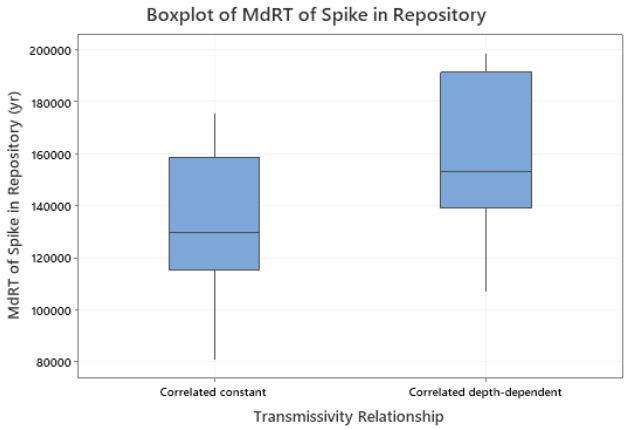

Figure 7. Box plot showing the time when half the tracer is gone from the repository in years.

3.4. Fractional Mass Flux

Similarly, to both the maximum ^{129}I and MdRT results, the fractional mass flux from the repository shows similar results. As can be seen in Figure 8, there is a considerable amount of overlap between confidence intervals for the two transmissivity relationships. Additionally, the box plot in Figure 9 shows a large amount of overlap. However, the mean fractional mass flux for the CDD relationship is slightly lower which is expected given the results seen in Section 3.3.

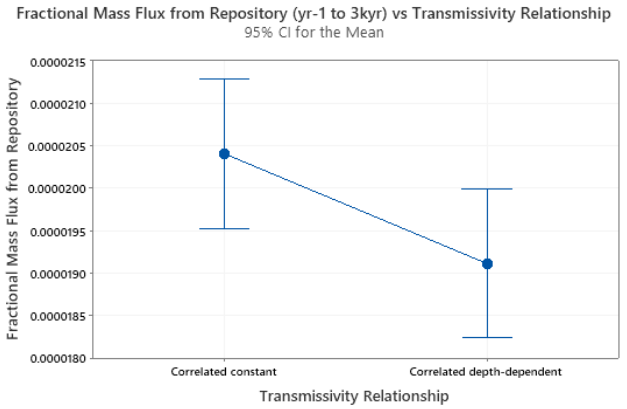

Figure 8 Interval plot for the fractional mass flux from the repository at 3 thousand years.

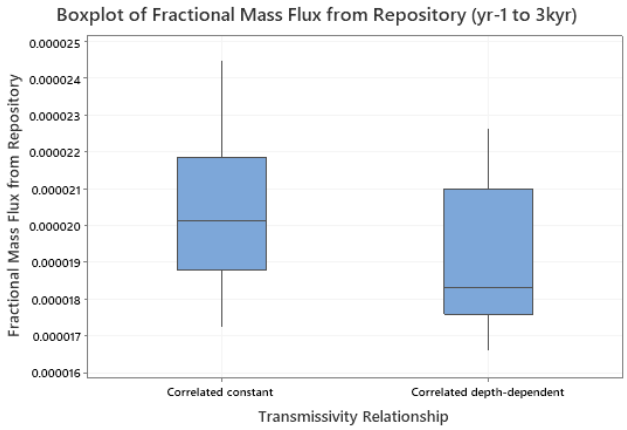

Figure 9 Boxplot for the fractional mass flux from the repository at 3 thousand years.

3.5. Mass Flow Rates

To further investigate the assumption that there will be an increase in downstream flow and little increase in vertical flow towards the aquifer for the CDD transmissivity relationship, the time history data for the mass flow rates was compared. Figures 10 and 11 below, which display the mass flow rate from the rock to east boundary, show a difference between the transmissivity relationships with no overlap of the 95% confidence intervals. The mean mass flow rate for the CC relationship is a little less than 90,000 kg/yr and the mean mass flow rate for the CDD relationships is around 1,000,000 kg/yr.

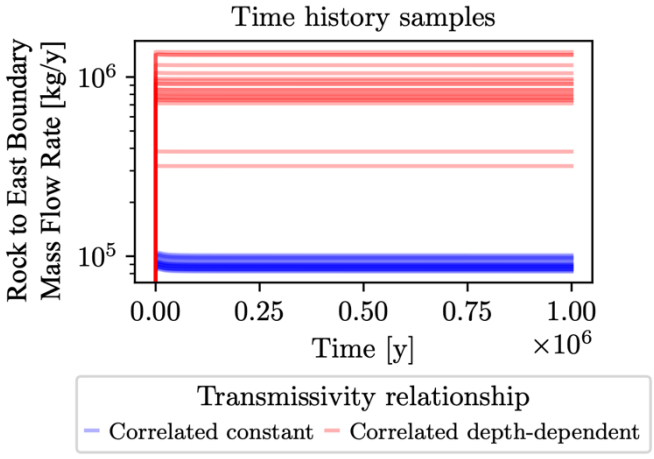

Figure 10. Mass flow rate [kg/yr] from the rock to east boundary over time.

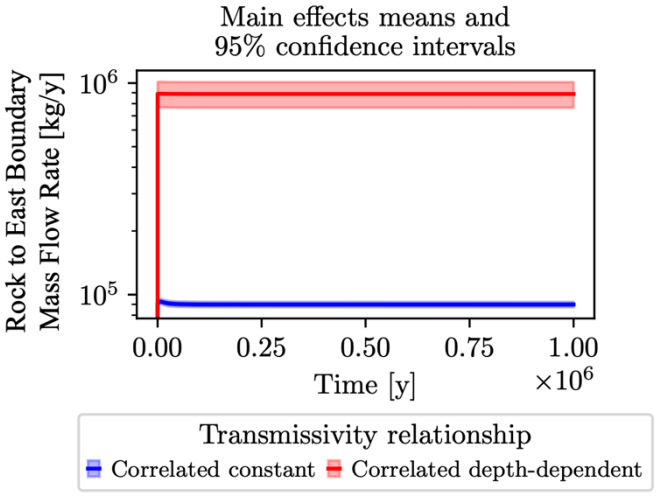

Figure 11. Main effects plot for the mass flow rate [kg/yr] from the rock to the east boundary over time.

Figures 12 and 13 represent the mass flow rate from the rock to the aquifer over time. As can be seen in Figure 12, the mean mass flow rates for the two relationships are similar, but the CDD relationship mass flow rates range from 1,000,000 kg/yr to -1,000,000 kg/yr (a negative flow rate indicates a reverse in flow from the aquifer to the rock). This large range is what is influencing the large 95% confidence intervals in Figure 13. These results coincide with the expected effect of transmissivity relationship on the streamwise flow rate and vertical flowrates, which were discussed at the end of Section 3.1.

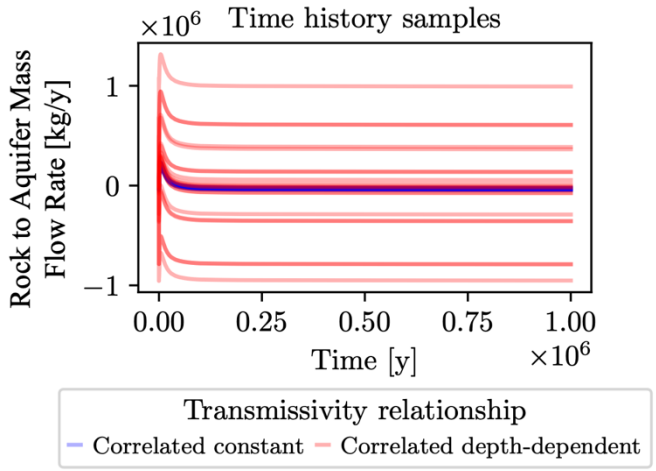

Figure 12. Mass flow rate [kg/yr] from the rock to aquifer over time.

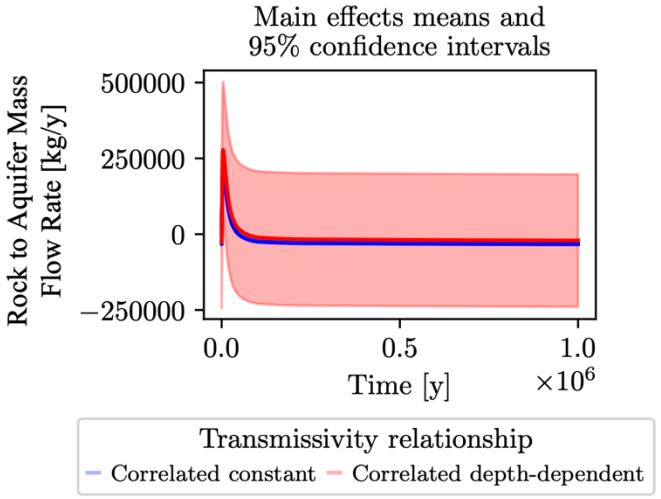

Figure 13. Main effects plot for the mass flow rate [kg/yr] from the rock to aquifer over time.

4. DISCUSSION

In conclusion, the purpose of this study was to determine if a correlated depth-dependent transmissivity relationship produces a significant change in the performance quantities for the flow and transport simulations of nuclear repositories in subsurface rock. The results indicated a statistically significant difference for the permeabilities of each depth zone and the mass flow rate from the rock to east boundary. The other QoIs examined showed no statistically significant difference in means between the two transmissivity relationships. It was quite unexpected that the depth-dependent transmissivity relationship did not strongly influence a change in these quantities. However, the statistically significant difference for the rock to east boundary flow rate may indicate increased flushing for the CDD relationship meaning the ^{129}I is not reaching the aquifer. This behavior is worth further investigation. Additionally, it is worth identifying what factors are influencing the

extreme maximum ^{129}I case shown in Figure 3 as well as determining why there is such a large range for the CDD relationship rock to aquifer mass flow rate. These are planned as part of future investigations.

ACKNOWLEDGEMENTS

This work has been performed as part of the Geologic Disposal Safety Assessment program. Sandia National Laboratories is a multimission laboratory managed and operated by National Technology & Engineering Solutions of Sandia, LLC, a wholly owned subsidiary of Honeywell International Inc., for the U.S. Department of Energy's National Nuclear Security Administration under contract DE-NA0003525. This paper describes objective technical results and analysis. Any subjective views or opinions that might be expressed in the paper do not necessarily represent the views of the U.S. Department of Energy or the United States Government. SAND2022-XXXX C

REFERENCES

1. Hyman, J. D., S. Karra, N. Makedonska, C. W. Gable, S. L. Painter and H. S. Viswanathan (2015). "dfnWorks: A discrete fracture network framework for modeling subsurface flow and transport," *Computers & Geoscience*, **84**:10-19.

2. IAEA (International Atomic Energy Agency) 2012. The Safety Case and Safety Assessment for the Disposal of Radioactive Waste, Specific Safety Guide. *IAEA Safety Standards Series* No. SG-23, IAEA, Vienna, Austria.

3. Lichtner, P. C. and G. E. Hammond (2012). Quick Reference Guide: PFLOTRAN 2.0 (LA-CC-09-047) Multiphase-Multicomponent-Multiscale Massively Parallel Reactive Transport Code. LA-UR-06-7048. Los Alamos National Laboratory, Los Alamos, New Mexico.

4. Mariner, P., M. Nole, E. Basurto, T. M. Berg, K. W. Chang, B. Debusschere, A. C. Eckert, M. S. Ebeida, M. B. Gross, and G. Hammond (2020). "Advances in GDSA Framework Development and Process Model Integration." Sandia National Lab.(SNL-NM), Albuquerque, NM (United States); Sandia …, https://doi.org/10.2172/1671380.

5. NEA (Nuclear Energy Agency) 2013. The Nature and Purpose of the Post-Closure Safety Cases for Geological Repositories, NEA/RWM/R(2013)1, Organisation for Economic Cooperation and Development, *Nuclear Energy Agency*, Paris, France.

6. Rechard, R. P., T. A. Cotton, and M. D. Voegele 2014. "Site selection and regulatory basis for the Yucca Mountain disposal system for spent nuclear fuel and high-level radioactive waste." *Reliability Engineering & System Safety*, 122, 7-31. doi: 10.1016/j.ress.2013.06.021

7. Stein, E., J. M. Frederick, G. E. Hammond, K. L. Kuhlman, P. Mariner, and S. D. Sevougian (2017). "Modeling Coupled Reactive Flow Processes in Fractured Crystalline Rock." In Proceedings of the 16th International High-Level Radioactive Waste Management Conference. Charlotte, North Carolina. https://www.osti.gov/servlets/purl/1417242.

8. Joyce, S., L. Hartley, D. Applegate, J. Hoek, and P. Jackson (2014). Multi-scale groundwater flow modeling during temperate climate conditions for the safety assessment of the proposed high-level nuclear waste repository site at Forsmark, Sweden. *Hydrogeology Journal*, 22(6):1233–1249.